



A Computational Study of UDCA and TUDCA as Novel Therapeutic Agents for Parkinson's Disease

Aswin Krishnamurthy, Nandhini Sundaresan*, Vivekananthan Govindaraj, Sanjay Raamakrishnan, Monish Janarthanan

Department of Pharmacognosy, Sri Ramachandra Faculty of Pharmacy, Sri Ramachandra Institute of Higher Education and Research, Porur, Chennai 600 116, Tamil Nadu, India

*Corresponding Author's Email: nandypharma1787@gmail.com

Abstract

Parkinson's disease (PD) is a progressive neurodegenerative disorder characterised by the loss of dopamine-producing neurons in the brain, resulting in motor disturbances such as tremors, rigidity, and slowed movement. Although current therapies can improve symptoms, many patients experience side effects and a gradual decline in treatment effectiveness over time. This study employs comprehensive *in silico* methods to evaluate the therapeutic potential of ursodeoxycholic acid (UDCA) and tauroursodeoxycholic acid (TUDCA), two bile acids with emerging neuroprotective properties. Molecular docking studies were conducted using AutoDock 1.5.7 software, and the ADMET properties of the compounds were assessed using SwissADME. Toxicity analyses of UDCA and TUDCA were performed using T.E.S.T 5.1.2 software. Molecular dynamics (MD) simulations of UDCA–protein complexes were carried out via the iMOD server and CABS-flex V 2.0. Molecular docking simulations revealed promising interactions between UDCA and TUDCA with Parkinson's disease-associated proteins selected from the literature, including 1XQ8, 6CM4, 6RKB, and 4PYK. UDCA generally exhibited stronger binding affinities of -5.38 , -8.99 , -8.21 , and -6.50 kcal/mol compared to TUDCA (-5.08 , -7.07 , -8.30 , -5.94 kcal/mol), except in the case of MAO-B. Molecular dynamics simulations further supported the stability of the UDCA–protein complexes, with eigenvalues calculated as 3.97×10^{-7} , 2.39×10^{-6} , 1.59×10^{-5} , and 9.02×10^{-5} . Pharmacokinetic analyses indicated favourable properties for both UDCA and TUDCA, including high oral bioavailability and blood–brain barrier permeability. UDCA displayed slightly higher toxicity in aquatic organisms but exhibited comparable developmental and mutagenic risks to TUDCA. Collectively, these computational findings highlight the multi-target potential of UDCA and TUDCA in modulating neuroinflammatory processes, mitigating oxidative stress, and supporting mitochondrial integrity—mechanistic pathways central to PD pathogenesis.

Keywords: Molecular Docking; Mitochondrial Dysfunction; Neurodegeneration; Parkinson's Disease; Taurodeoxycholic Acid; Ursodeoxycholic Acid

Introduction

Parkinson's disease, a progressive neurodegenerative disorder, stealthily encroaches upon the body's intricate network of movement and control. As this insidious condition advances, it gradually diminishes the brain's ability to produce dopamine, a vital neurotransmitter that orchestrates smooth and coordinated movements (Vastegani *et al.*, 2023). Alpha-synuclein (α -syn) amyloid, also known as Lewy bodies, accumulates in the nerve terminals and causes severe damage to dopaminergic neurons in the substantia nigra by increasing the production of mitochondrial reactive oxygen species (ROS) and decreasing protein synthesis, thereby promoting mitochondrial DNA damage (Zong *et al.*, 2024; Lim & Klein, 2024). Bradykinesia, stiffness, postural instability, and resting tremor are the hallmark motor symptoms observed in patients with PD. Furthermore, many non-motor characteristics of PD are also

well recognised, such as loss of smell, depression, hyposmia, dementia, and pain (Sveinbjornsdottir, 2016). As life expectancies rise and competing causes of death decline, the prevalence of Parkinson's disease is predicted to reach between 12 and 17 million by 2040. An increase of this magnitude would necessitate additional personnel and medical resources, thereby intensifying the burden currently placed on health systems across the world (Váradi, 2020; Guglietti *et al.*, 2024). Although the exact aetiology of PD remains unknown, experts suspect it involves both genetic and environmental factors. In addition to exposure to certain chemicals, pesticides, and solvents, individuals with a family history of PD are at an increased risk of developing the disease.

Currently, the only available treatment for PD focuses on alleviating its symptoms. Research on PD is primarily directed towards developing disease-modifying drugs that can halt or slow the underlying neurodegenerative process (Armstrong & Okun, 2020). The principal aim of pharmacological therapy in PD is to increase dopamine levels in the brain or to mimic its effects. The most commonly used medications include Levodopa, dopamine agonists (ropinirole, pramipexole, rotigotine), MAO-B inhibitors (selegiline, rasagiline), COMT inhibitors (entacapone, tolcapone), anticholinergics (trihexyphenidyl, benztropine), and amantadine (Stoker & Barker, 2020). Surgical procedures, including Deep Brain Stimulation (DBS) and lesioning techniques, are also employed in PD management (Sharma *et al.*, 2020). Deep Brain Stimulation (DBS) has proven to be an effective treatment for managing motor symptoms in PD. Findings from several clinical studies have demonstrated that DBS targeting the internal segment of the globus pallidus or the subthalamic nucleus is effective in treating mild to severe cases of PD (Groiss *et al.*, 2009).

The neuroprotective mechanisms of UDCA and TUDCA—which include anti-apoptotic, anti-inflammatory, antioxidant, and mitochondrial-stabilising actions—make them effective treatment options for Parkinson's disease (Qi *et al.*, 2021; Vang *et al.*, 2014). Ursodeoxycholic acid (UDCA) is a hydrophilic, tertiary bile acid produced endogenously by the liver. UDCA is the drug of choice approved by the US Food and Drug Administration for the treatment of primary biliary cirrhosis and is widely used, non-toxic, and promotes the programmed cell death of lipophilic bile acids such as taurochenodeoxycholic acid and glycochenodeoxycholic acid (Kim *et al.*, 2018; Zhang *et al.*, 2019). UDCA possesses antioxidant properties that may reduce the formation of reactive oxygen species (ROS) in neurons, thereby decreasing oxidative stress and its damaging cellular effects. It has been demonstrated that UDCA enhances cellular energy production, which is crucial for neuronal function as neurons require substantial energy to operate effectively. It is proposed that by promoting mitochondrial biogenesis and inhibiting mitochondrial apoptosis, or cell death, UDCA improves mitochondrial function (Junior *et al.*, 2020).

According to recent research, tauroursodeoxycholic acid (TUDCA), a derivative of UDCA, prevents not only the death of hepatic cells but also the formation of oxygen radicals and apoptosis in non-hepatic cells, such as neural cells (Castro-Caldas *et al.*, 2012). TUDCA possesses anti-inflammatory properties and inhibits pro-inflammatory cytokines in the brain, which can help to slow the progression of neurodegeneration. However, the precise mechanisms by which UDCA and TUDCA prevent mitochondrial membrane disruption in general, and the permeability transition (PT) linked to apoptosis in particular, remain unclear. It has been demonstrated that TUDCA exhibits a strong capacity to counteract endoplasmic reticulum (ER) stress, a crucial stage in many forms of cellular dysfunction. As a result, TUDCA appears to act as a key signalling molecule in numerous cellular processes across various tissues. Nevertheless, translation to clinical therapy has been delayed, as the exact pathways and molecular signalling mechanisms through which these bile acids function are still not fully understood. Pathologically, alpha-synuclein aggregation is a hallmark of PD and has been shown to be reduced by UDCA and TUDCA, which may help maintain neuronal integrity and function (Bose & Beal, 2016). Difficulties in diagnosing PD, particularly in its early stages, further impede the implementation of effective therapies (Exner *et al.*, 2012).

This study builds upon prior evidence by employing robust in-silico approaches, including molecular docking, molecular dynamics simulations, and comprehensive ADMET (absorption, distribution, metabolism, excretion, and toxicity) profiling to quantitatively assess the binding interactions, stability,

and drug-likeness of UDCA and TUDCA against key PD-associated protein targets. By integrating data on binding affinities, pharmacokinetic properties, and safety profiles, this research aims to clarify the mechanistic underpinnings and translational prospects of these compounds as candidate neuroprotective agents for PD. In doing so, the study contributes important computational insights to the field, helping to guide future experimental and clinical investigations directed at disease modification in Parkinson's disease.

Materials and Methods

Ligands and Protein Preparation

The 3D structure of UDCA (CID:3401) and TUDCA (CID:9848818) obtained from PubChem in SDF format, a compound database (<https://pubchem.ncbi.nlm.nih.gov/>) (Kim *et al.*, 2023), and used Open Babel to convert it into MOL2 format (O'Boyle *et al.*, 2011). In this work, the molecular docking of UDCA and TUDCA was carried out towards the PDB IDs: 1XQ8, 6CM4, 6RKB, and 4PYK originated from the RCSB Protein Data Bank and were downloaded directly (PDB) (<https://www.rcsb.org/>) (Berman *et al.*, 2000). The protein is selected based on the literature search depicted in Table 1. Using BIOVIA Discovery Studio Visualiser, unnecessary structures and nonstandard residues were removed from proteins that were obtained from the PDB (Sharma *et al.*, 2019). Ligand preparation and target identification flow-chart depicted in Figure 1.

Table 1: Key Protein Targets for Molecular Docking in Parkinson's Disease

Protein Target	Role in Parkinson's Disease	Justification for Selection	References
Alpha-synuclein (ASN)	Forms Lewy bodies; mediates neurotoxicity	Central in PD pathology via toxic aggregation and oxidative stress	Bartels <i>et al.</i> , 2011
Dopamine D2 receptor (D2R)	Regulates motor control signaling	Key receptor in dopaminergic signaling; target for symptom relief	Kaasinen <i>et al.</i> , 2003
Monoamine oxidase B (MAO-B)	Dopamine catabolism is, source of oxidative stress	The target of MAO-B inhibitors that reduce dopamine breakdown	Teo & Ho, 2013; Jost, 2022
Catechol-O-methyltransferase (COMT)	Controls dopamine metabolism	COMT inhibition augments the levodopa effect, improves dopamine availability	Kwak <i>et al.</i> , 2024

Molecular Docking Analysis

AutoDock 4.2 was used to do the docking studies of UDCA and TUDCA with the target proteins (<https://autodock.scripps.edu/>) (Morris *et al.*, 2009). Proteins and ligands were augmented with polar hydrogen and Kollman charges. To determine ligand-protein binding energies, the grid box coordinates of enclosed protein were fixed. 20 runs were produced for every ligand-protein interaction. Every ligand-protein combination that might exist was created as a compound. A pose was chosen and exported from the complex that had the lowest binding energy. Ultimately, the BIOVIA Discovery Studio Visualiser 4.5 was utilised to identify and visualise the interaction between the protein and ligand through 2-D and 3-D images.

Molecular Dynamics Simulation

Protein-ligand complex stability was evaluated using molecular dynamics (MD) simulations. Using the iMOD server (<https://imods.igf.csic.es/>) (López-Blanco *et al.*, 2011) and CABS-flex V 2.0 (<http://biocomp.chem.uw.edu.pl/CABSflex2>) (Kuriata *et al.*, 2018), MD simulations were carried out. Using CABS-flex, every protein's structural flexibility (RMSF) was evaluated. In iMOD, the remaining parameters were maintained at their standard configurations, and the time of simulation was changed

to 10 ns. Docketed PDB files were employed in the input files. Every parameter in the file was submitted to the iMODS server with its default settings.

ADME and Drug-Likeness Prediction

SwissADME (<http://www.swissadme.ch/>), created by the Swiss Institute of Bioinformatics (Daina et al., 2017), was used to carry out the *in-silico* ADME screening and drug-likeness assessment. The US Environmental Protection Agency offers free software called Toxicity Estimation Software Tool (T.E.S.T.) was used for toxicity analysis for UDCA and TUDCA.

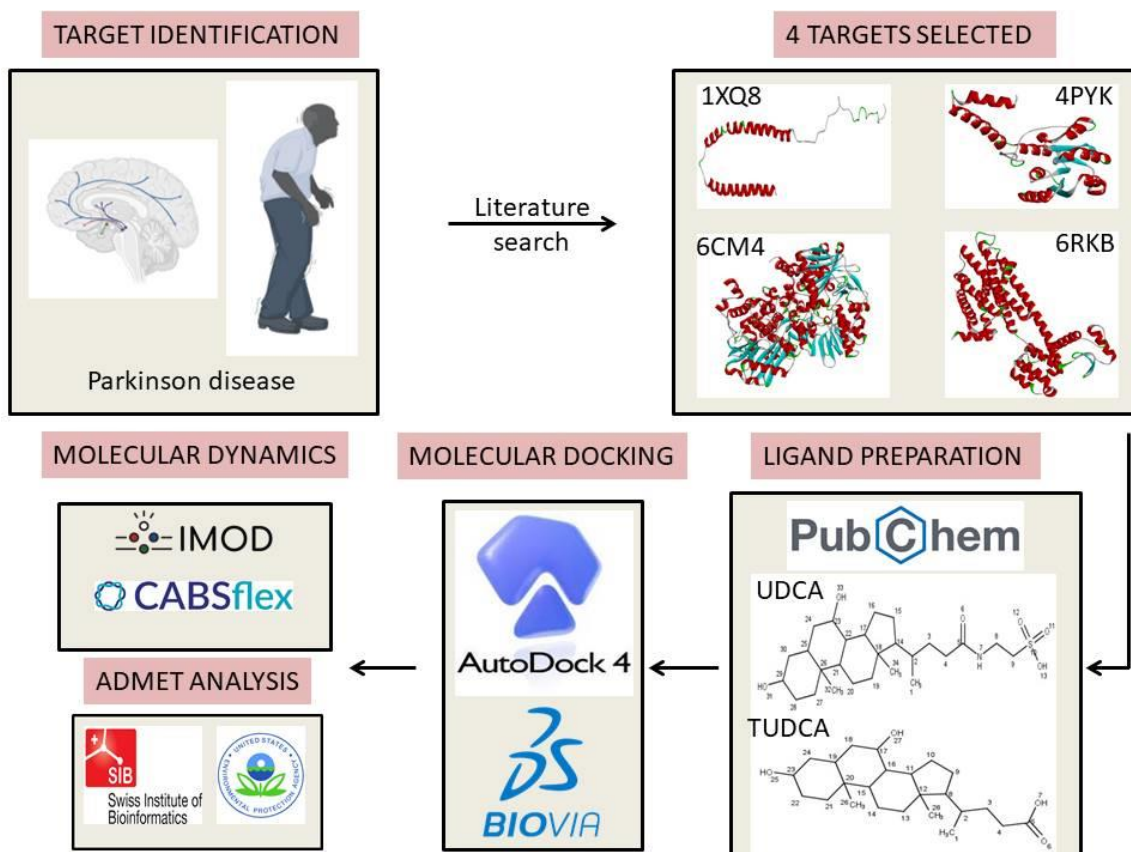


Figure 1: Flow Chart for Target Identification and Ligand Preparation

Result

Pharmacological targets for modifying PD may include neuronal inflammation, mitochondrial dysfunction, oxidative stress, calcium (Ca^{2+}) channel activity, leucine-rich repeat kinase 2 (LRRK2) gene activity, and α -synuclein accumulation, aggregation, and intercellular transmission (immunotherapy approaches) (Connolly & Lang, 2014). Table 2 illustrates the interactions of ASN, D2, MAO-B, and COMT with UDCA and TUDCA. Docking studies indicate that both ursodeoxycholic acid (UDCA) and tauroursodeoxycholic acid (TUDCA) exhibit distinct binding patterns towards four selected proteins associated with neurodegenerative diseases. The findings reveal notable differences in their binding affinities and molecular interactions, which may enhance their therapeutic potential.

With respect to alpha-synuclein (ASN), UDCA demonstrated a stronger binding propensity (-5.38 kcal/mol) than TUDCA (-5.08 kcal/mol), as depicted in Figure 2. Both ligands shared common interaction sites at LYS43, TYR39, and GLU35; however, UDCA additionally interacted with THR33 and LYS32. These supplementary interactions may account for UDCA's stronger binding affinity and potentially greater efficacy in reducing alpha-synuclein aggregation—a defining pathological feature of Parkinson's disease. The most significant difference was observed in the binding pattern to the dopamine D2 receptor, where UDCA exhibited higher affinity (-8.99 kcal/mol) compared with TUDCA

(-7.07 kcal/mol), as shown in Figure 3. UDCA binds to the orthosteric binding pocket of the receptor and interacts with key residues located at the end of the pocket, including HIS393, PHE389, and TYR416. Both UDCA (-8.21 kcal/mol) and TUDCA (-8.30 kcal/mol) demonstrated nearly identical binding affinities for MAO-B, suggesting that these bile acids interact similarly with this target (Figure 4). While minor differences in residue interactions may reflect slight variations in their binding poses, the overall interaction strength remains comparable. UDCA also showed favourable binding affinity with COMT (PDB: 4PYK), registering a value of -6.50 kcal/mol compared with TUDCA (-5.94 kcal/mol), as depicted in Figure 5. Therefore, UDCA may possess the potential to inhibit peripheral COMT activity, thereby enhancing dopamine concentrations.

Table 2: Binding Affinities and Interaction of UDCA And TUDCA with Target Proteins

Sl.No	Target	Protein Data Bank	Binding affinities (kcal/mol) of UDCA	Residues in contact with UDCA	Binding affinities (kcal/mol) of TUDCA	Residues in contact with TUDCA
1.	ASN	1XQ8	-5.38	LYS43,LEU38,VAL40,TYR39,LYS45,THR33,LYS32,GLY36,GLU35	-5.08	LYS45,VAL48,THR44,LYS43,VAL40,TYR39,GLU35,LEU38,GLY36
2.	D2	6CM4	-8.99	HIS393,PHE189,PHE198,VAL115,VAL111,VAL190,ALA122,PHE382,SER121,CYS118,THR119,PHE390,SER197,TRP386,SER193,ASP114,TYR416,THR412,PHE389,ILE184,TYR408	-7.07	VAL159,ILE158,ALA127,VAL154,ARG151,MET155,ILE130,CYS126,LEU123,LEU162,VAL204,VAL200,VAL196,PRO201,ILE166
3.	MAO-B	6RKB	-8.21	GLU303,LYS302,LYS52,TYR332,ASN336,LYS50,TYR300,ALA339,ALA338,TYR301,VAL381	-8.30	PRO102,GLY101,PHE99,ARG100,PRO105,TYR112,VAL106,HIS115,TRP119,LEU164,PRO104,ASN116,PHE103,GLU483
4.	COMT	4PYK	-6.50	ASN220,LYS96,HIS243,ASP219,VAL221,TYR244,ILE99,LEU217,ALA218,ILE222,GLN245,MET90,SE R246,PHE247,LYS55,LEU248,CYS223	-5.94	CYS238,LEU210,ARG211,PHE239,THR214,GLU240,GLY213,VAL215,LYS212

ASN- α -synuclein, D2- Dopamine receptor, MAO-B- Monoamine oxidase type-B, COMT- Catechol O-methyltransferase

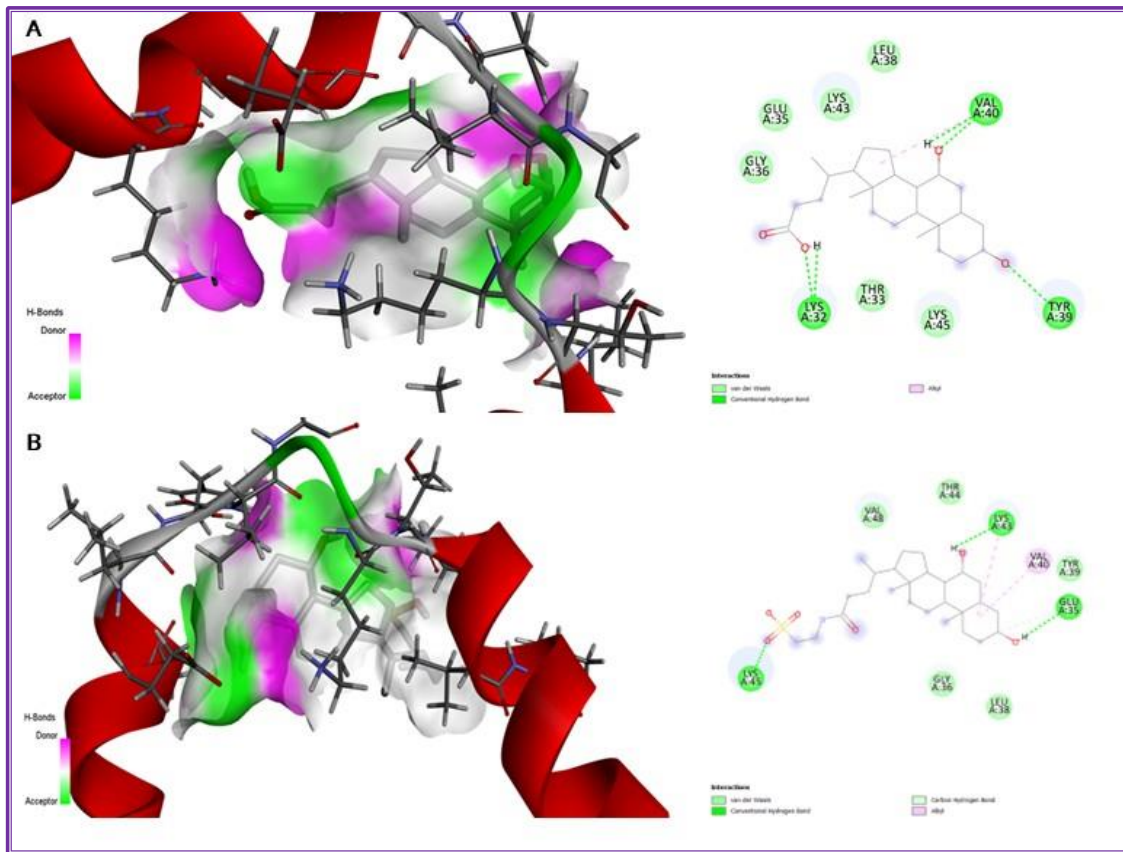


Figure 2: 2D and 3D image of 1XQ8 with (A) UDCA, (B) TUDCA

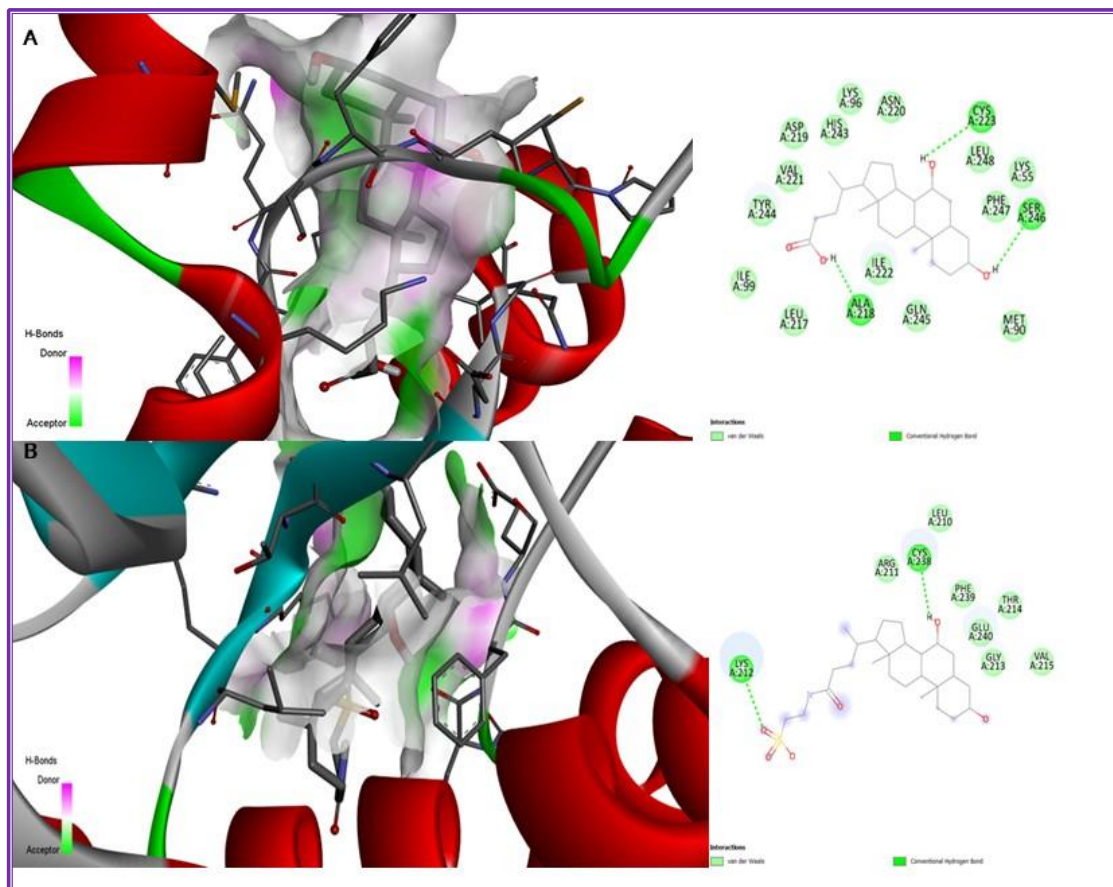


Figure 3: 2D and 3D image of 4PYK with (A) UDCA, (B) TUDCA

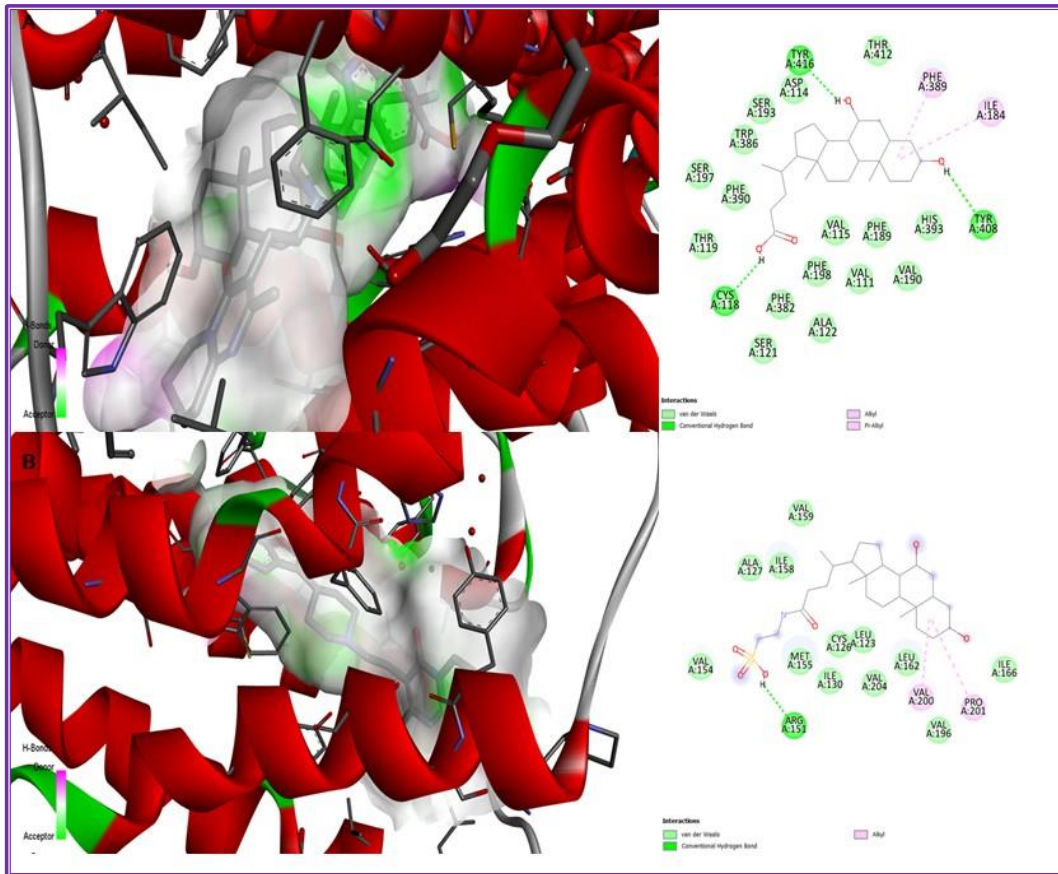


Figure 4: 2D and 3D image of 6CM4 with (A) UDCA, (B) TUDCA

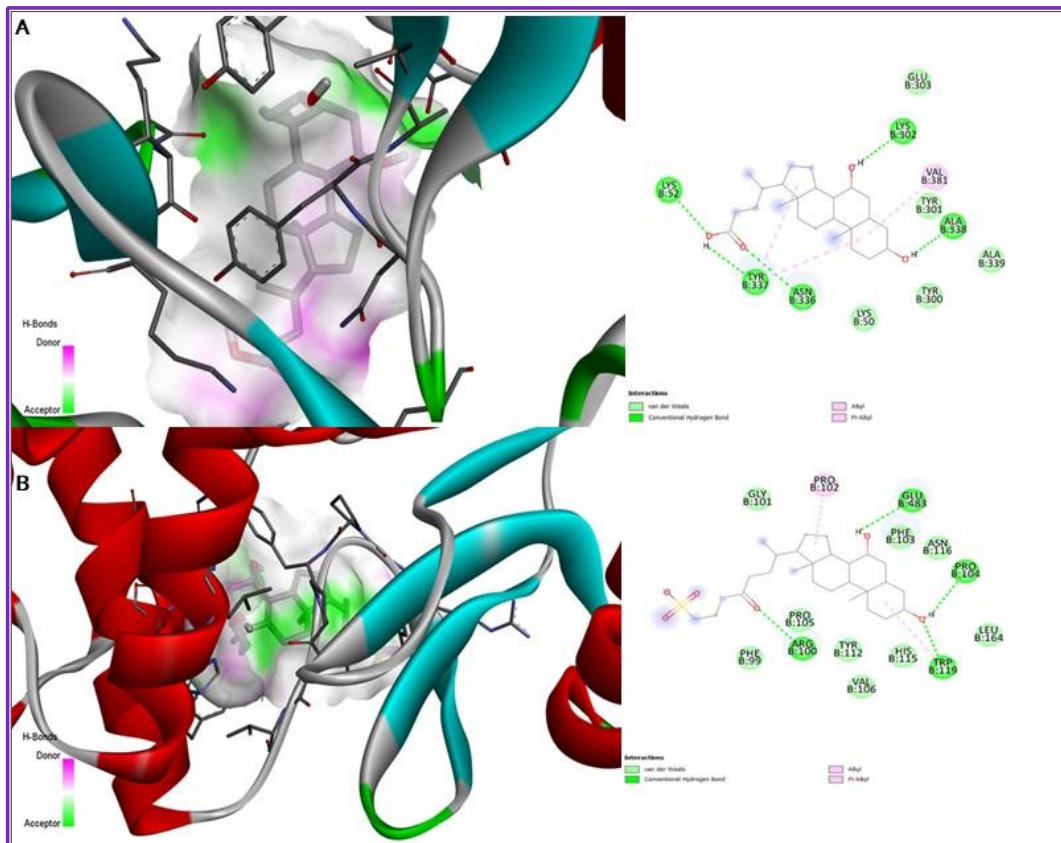


Figure 5: 2D and 3D image of 6RKB (B CHAIN) with (A) UDCA, (B) TUDCA

Molecular Dynamics

The stability of the highest-ranked docked complexes was determined using the iMODS server through internal coordinate analysis and Normal Mode Analysis (NMA). Molecular dynamics simulations were performed only for the UDCA–protein complexes due to their higher binding affinities compared to TUDCA. Several parameters, including B-factors, deformability, eigenvalues, covariance maps, and elastic network models, were evaluated and presented graphically to assess stability. In the four protein complexes, molecular dynamics simulations were assessed using CABS-flex, which revealed that each of the four proteins displayed flexibility in their RMSD peaks, indicating the minimum value to which the system was constrained during the simulation. Table 3 presents the eigenvalues and deformability of the protein–UDCA complexes. According to the RMSD data (Figure 6), these protein–UDCA complexes exhibit a trend of increasing structural stiffness and decreasing flexibility as eigenvalues increase ($1XQ8 < 4PYK < 6CM4 < 6RKB$). Variance decreases with increasing eigenvalues and vice versa, as less fluctuation occurs when energy is concentrated in fewer modes. Among the proteins analysed, 1XQ8 had the lowest eigenvalue (3.97×10^{-7}), indicating the greatest flexibility, whereas 6RKB (B chain), with the highest eigenvalue (9.02×10^{-5}), was the most rigid in complex with UDCA (Figure 7). The B-factor represents the flexibility and dynamics of protein structures by comparing theoretical NMA predictions with experimental PDB data. This comparison provides insights into both local (atomic-level) and global (collective) molecular motions, as illustrated in Figure 8. The variance plots (Figure 9) display how much of the total molecular motion is captured by the first 20 modes in the NMA for each protein. The variance and eigenvalues corresponding to each normal mode are inversely correlated. The individual (red) and cumulative (green) deviations are represented by coloured bars. The 1XQ8 protein exhibited the greatest deformability, with a value of 0.521 (Figure 10), indicating that 1XQ8 possesses the highest flexibility among the protein–UDCA complexes. The covariance matrix illustrates how pairs of residues are coupled, showing whether their movements are uncorrelated (white), correlated (red), or anti-correlated (blue), as shown in Figure 11. In the elastic network model, dots are coloured according to their stiffness—darker grey dots represent stiffer springs, whereas lighter shades indicate more flexible regions.

Table 3: Eigenvalue and Deformability of Protein-UDCA Complexes

Protein-UDCA complex	Eigenvalue	Deformability
1XQ8	3.97×10^{-7}	0.521
4PYK	2.39×10^{-6}	0.0273
6CM4	1.59×10^{-5}	0.0023
6RKB (B CHAIN)	9.02×10^{-5}	0.0054

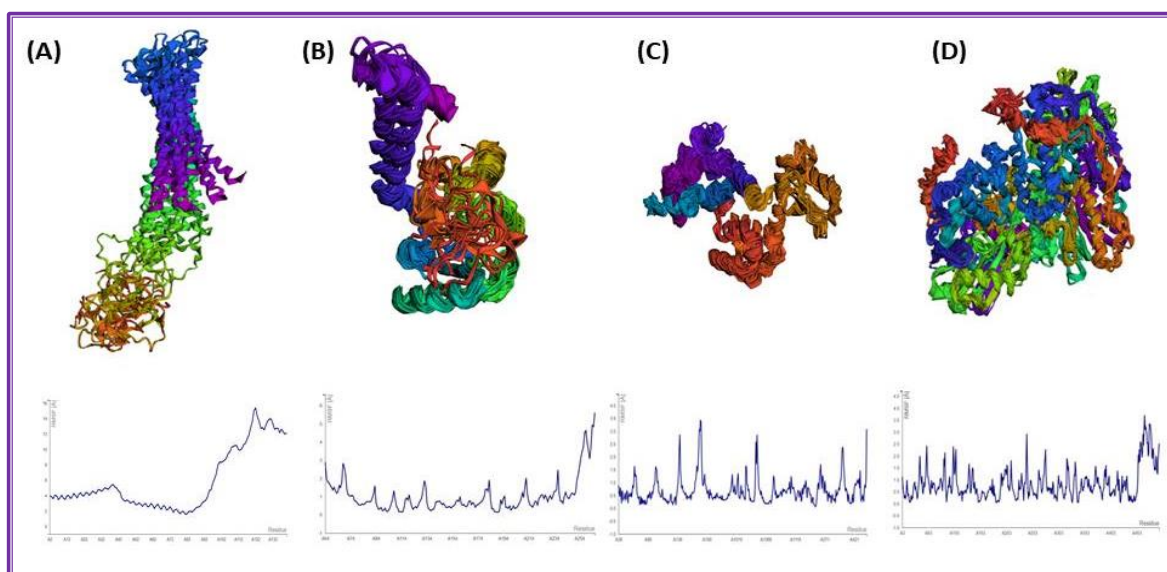


Figure 6: MD Simulation of Multimodel Superimposed Structure and RMSD Of (A) 1XQ8, (B) 4PYK, (C) 6CM4, (D) 6RKB

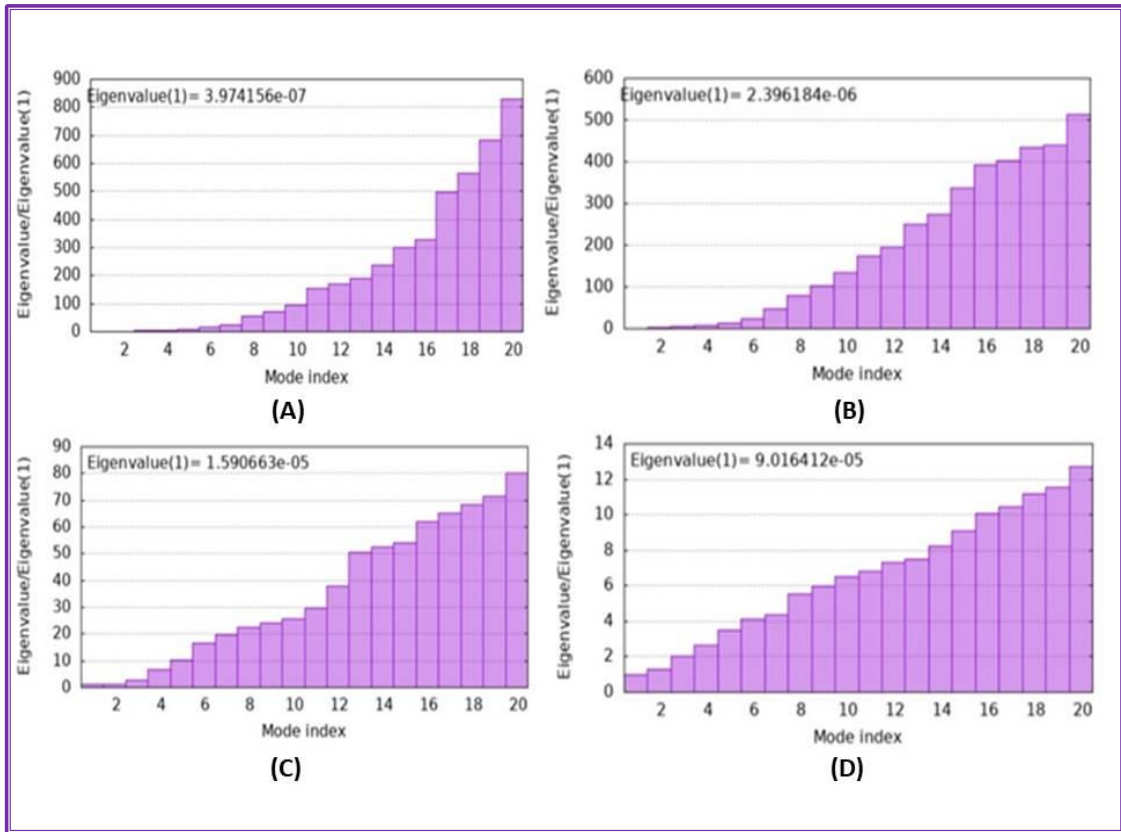


Figure 7: Eigenvalue (A) 1XQ8 (B) 4PYK (C) 6CM4 (D) 6RKB

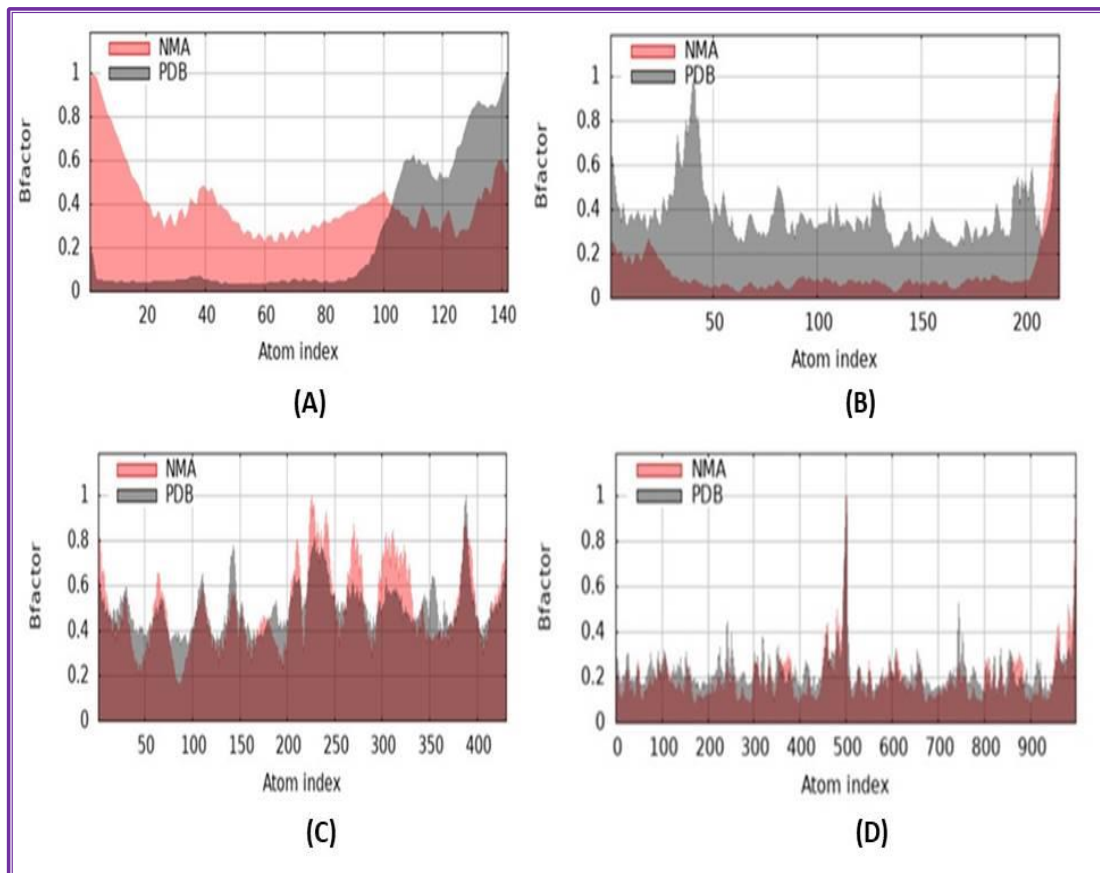


Figure 8 : B-factor (A) 1XQ8 (B) 4PYK (C) 6CM4 (D) 6RKB

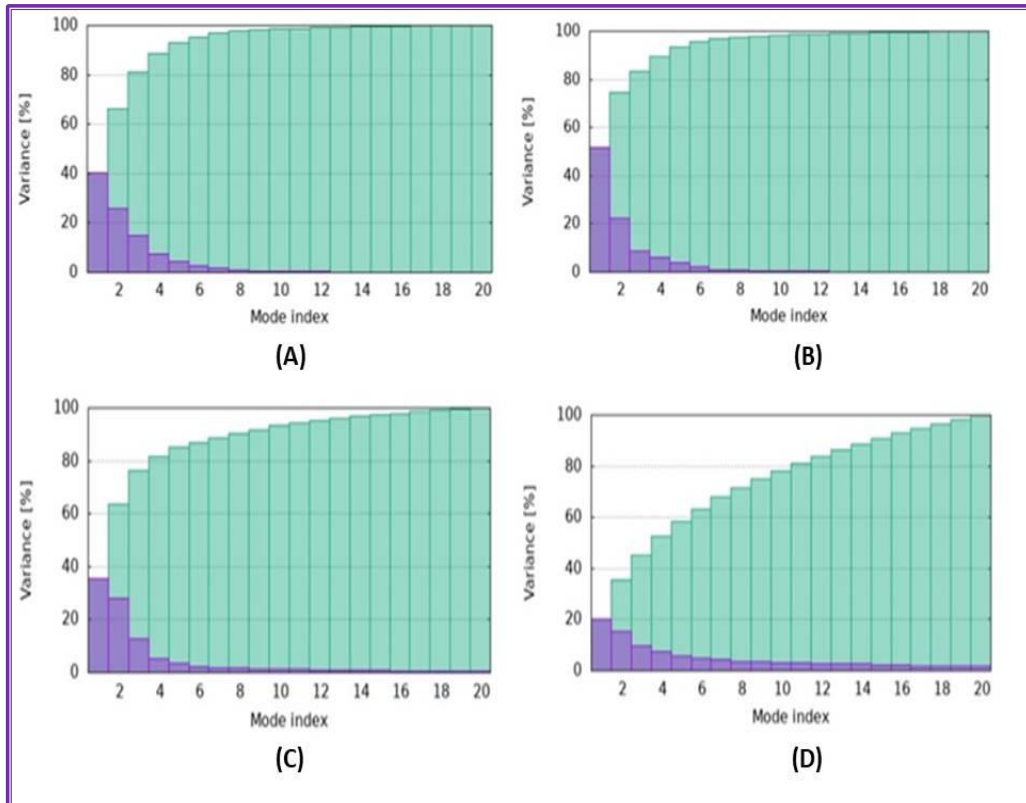


Figure 9: Variance (%) (A) 1XQ8 (B) 4PYK (C) 6CM4 (D) 6RKB

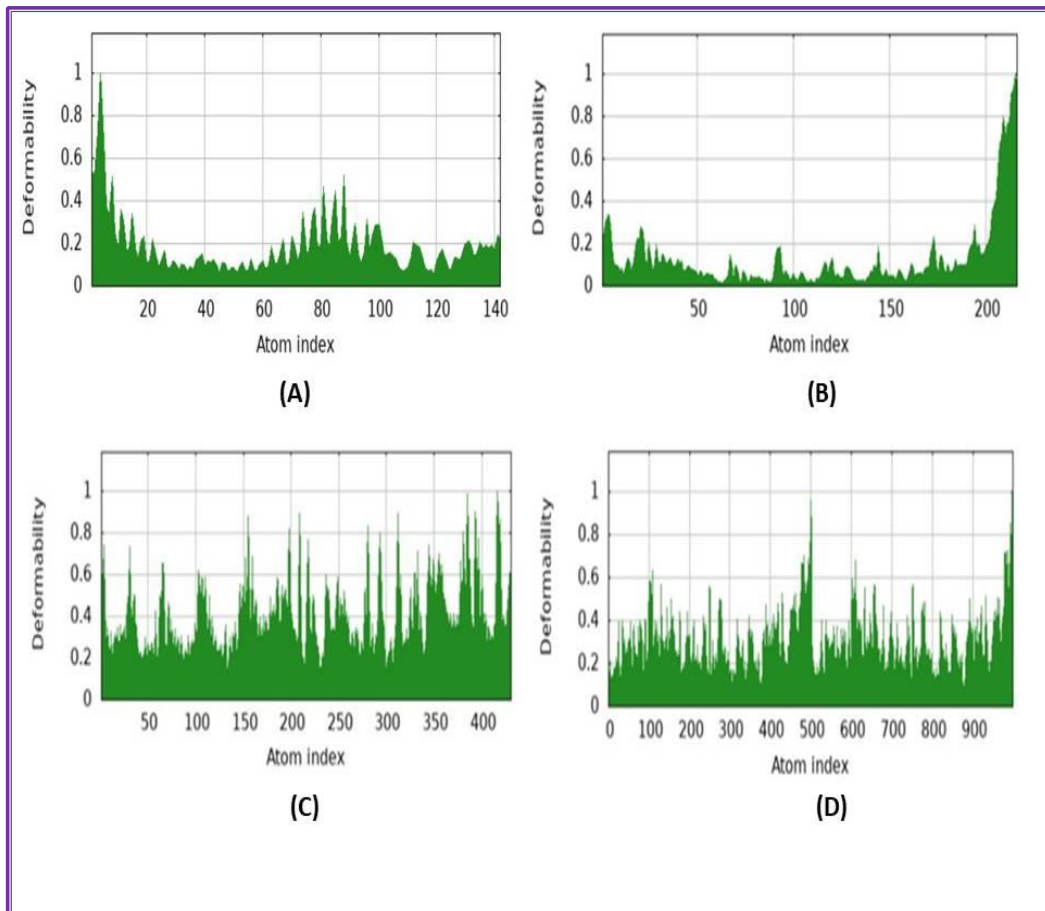


Figure 10: Deformability (A) 1XQ8 (B) 4PYK (C) 6CM4 (D) 6RKB

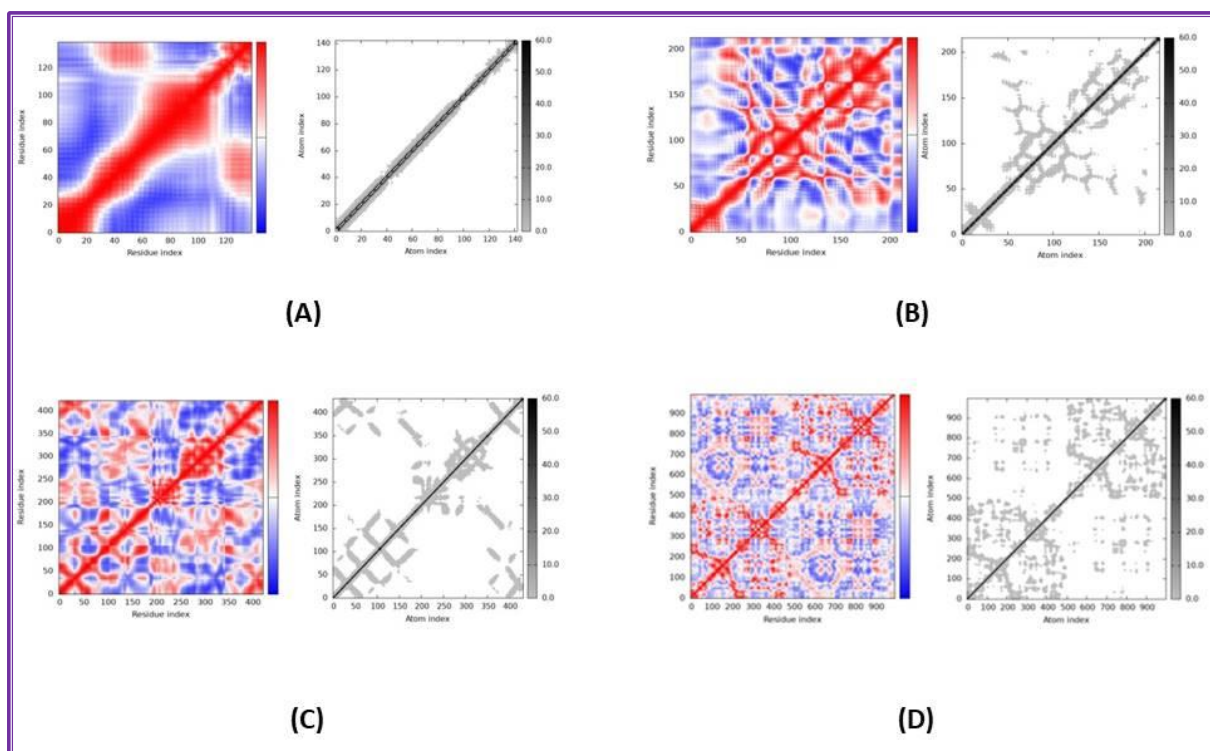


Figure 11: Covariance Map and Elastic Network
 network (A) 1XQ8 (B) 4PYK (C) 6CM4 (D) 6RKB

ADMET Analysis of UDCA and TUDCA

Table 4: Drug-likeness and Pharmacokinetic Properties of UDCA and TUDCA

Druglikeness and Pharmacokinetic Property	UDCA	TUDCA
Lipinski	Yes, 0 violations	Yes, 0 violations
Ghose	Yes	No; 3 violations: MW>480, MR>130, #atoms>70
Veber	Yes	Yes
Egan	Yes	No, 1 violation: TPSA>131.6
Muegge	Yes	Yes
GI absorption	High	Low
BBB Permeability	Yes	Yes
P-gp substrate	Yes	Yes
CYP1A2 inhibitor	No	No
CYP2C19 inhibitor	No	No
CYP2C9 inhibitor	No	No
CYP2D6 inhibitor	No	No
CYP3A4 inhibitor	No	Yes

Table 5: The Estimated Toxicity Values of UDCA And TUDCA Using T.E.S.T Version 5.1.2

Parameters	UDCA	TUDCA
Oral rat LD50	4602.51 mg	-
Fathead minnow LD50 (96hr)	1.12 mg/L	2 mg/L
Daphnia magna LD50 (48hr)	9.27mg/L	-
Developmental toxicity	0.92 (+)	0.89 (+)
Ames mutagenicity	0.58 (+)	0.60 (+)

Table 4 presents the drug-likeness and pharmacokinetic properties of UDCA and TUDCA. The analysis of drug-likeness criteria and pharmacokinetics provides insight into their potential as therapeutic agents, particularly concerning oral bioavailability, absorption, and interactions with drug-metabolising enzymes. UDCA generally exhibits favourable drug-likeness and pharmacokinetic characteristics, including high oral absorption and blood–brain barrier (BBB) permeability, without significant inhibition of CYP enzymes. TUDCA, while demonstrating beneficial neuroprotective properties, shows certain limitations in drug-likeness due to lower oral bioavailability, higher molecular weight, and inhibition of CYP3A4. UDCA displays higher toxicity in aquatic organisms such as fathead minnows (1.12 mg/L) and *Daphnia magna* (9.27 mg/L) compared with TUDCA, as depicted in Table 5. Both compounds exhibit positive indications of developmental toxicity and mutagenicity; however, their scores are relatively close, suggesting comparable risk levels. The absence of oral LD₅₀ data for TUDCA restricts direct comparison of acute mammalian toxicity. Nonetheless, based on the available data, UDCA appears to be slightly more toxic in terms of aquatic toxicity and displays a higher developmental toxicity index than TUDCA.

Discussion

Table 4 presents the drug-likeness and pharmacokinetic properties of UDCA and TUDCA. The analysis of drug-likeness criteria and pharmacokinetics provides insight into their potential as therapeutic agents, particularly concerning oral bioavailability, absorption, and interactions with drug-metabolising enzymes. UDCA generally exhibits favourable drug-likeness and pharmacokinetic characteristics, including high oral absorption and blood–brain barrier (BBB) permeability, without significant inhibition of CYP enzymes. TUDCA, while demonstrating beneficial neuroprotective properties, shows certain limitations in drug-likeness due to lower oral bioavailability, higher molecular weight, and inhibition of CYP3A4. UDCA displays higher toxicity in aquatic organisms such as fathead minnows (1.12 mg/L) and *Daphnia magna* (9.27 mg/L) compared with TUDCA, as depicted in Table 5. Both compounds exhibit positive indications of developmental toxicity and mutagenicity; however, their scores are relatively close, suggesting comparable risk levels. The absence of oral LD₅₀ data for TUDCA restricts direct comparison of acute mammalian toxicity. Nonetheless, based on the available data, UDCA appears to be slightly more toxic in terms of aquatic toxicity and displays a higher developmental toxicity index than TUDCA.

Monoamine oxidase (MAO) is a riboflavin-containing protein located on the outer membrane of mitochondria. It catalyses the oxidative deamination of monoamine and tyramine neurotransmitters, including noradrenaline, dopamine, phenethylamine, and 5-hydroxytryptamine (Teo & Ho, 2013; Jost, 2022). There are two isoenzymes of MAO: MAO-A and MAO-B. Approximately 20% of the total MAO activity in the brain is attributed to MAO-A, while MAO-B accounts for about 80% (Robakis & Fahn, 2015). MAO-B is abundantly present in platelets and glial cells of the brain. As an adjunct to levodopa therapy, MAO-B inhibitors are often prescribed for PD patients who experience dyskinesia or motor fluctuations (Dezsi & Vecsei, 2017). Rasagiline and selegiline exhibit lower binding affinities with the MAO-B protein (PDB: 2C65) compared with UDCA and TUDCA (Gnanaraj et al., 2022). Catechol-O-methyltransferase (COMT) inhibitors are well established in the management of PD patients affected

by the wearing-off phenomenon (Kwak *et al.*, 2024). 3-O-methyldopa (3-OMD), a metabolite of levodopa, is catalysed by COMT (Müller, 2015). The central nervous system (CNS) and all peripheral tissues expressing COMT are crucial for determining levodopa bioavailability (Kwak *et al.*, 2024). In addition to reducing levodopa concentrations, peripheral COMT's product, 3-OMD, competes with levodopa for CNS dopamine uptake and blood–brain barrier transport, thereby impairing motor performance (Song *et al.*, 2021). UDCA and TUDCA exhibit lower binding affinities compared with the findings of Cruz-Vicente *et al.* (2021), where ZINC825166420 demonstrated higher binding affinity with MAO-B; thus, MAO-B may not represent a promising therapeutic target for PD.

Based on molecular docking studies, UDCA shows higher binding affinities with potential PD-related targets. TUDCA, a taurine-conjugated derivative of UDCA, shares a similar chemical structure but exhibits greater hydrophilicity and different membrane interaction properties. Consequently, molecular dynamics (MD) simulations focused solely on UDCA were conducted to reduce computational complexity and minimise bias introduced by conjugation effects. The molecular dynamics analysis revealed that UDCA induces varying degrees of stabilisation across protein targets, with α -synuclein (1XQ8) remaining the most flexible (eigenvalue 3.97×10^{-7}), while MAO-B (6RKB) was the most rigid (9.02×10^{-5}). The D2 receptor (6CM4) exhibited intermediate stability, suggesting that UDCA preserves the functional dynamics necessary for receptor modulation. Covariance maps indicated that UDCA maintains α -synuclein's correlated motions while restricting MAO-B's flexibility, demonstrating target-specific dynamic effects. ADMET analysis further revealed the pharmacokinetic potential of both UDCA and TUDCA.

Clinical studies investigating UDCA in the treatment of Parkinson's disease support the findings of the present research (Payne *et al.*, 2020; Sathe *et al.*, 2020; Zhu *et al.*, 2021). In contrast, there is currently no clinical evidence for TUDCA, although *in vitro* and preclinical studies provide valuable insights into its potential role in PD (Rosa *et al.*, 2018; Shtilbans *et al.*, 2024). Therefore, these results hold significant relevance, elucidating the molecular mechanisms underlying the potential targets of Parkinson's disease associated with UDCA and TUDCA.

Conclusion

The molecules UDCA and TUDCA are structurally similar and possess an exceptional ability to promote cell survival and enhance mitochondrial transcription, thereby increasing dopamine concentration. Overall, UDCA exhibits stronger or comparable binding affinities to the target proteins compared with TUDCA, except in the case of MAO-B, where TUDCA binds slightly more strongly. Molecular dynamics (MD) simulations of UDCA–protein complexes indicate that increasing eigenvalues are associated with reduced structural flexibility, signifying enhanced stability. Both compounds demonstrate good drug-likeness with minimal violations of key pharmacokinetic principles; however, TUDCA displays slightly greater deviations in medicinal chemistry parameters. Despite this, UDCA and TUDCA show comparable toxicity profiles in Ames mutagenicity and developmental toxicity assays. Given their low toxicity risks and favourable pharmacokinetic properties, both compounds represent promising candidates for further safety and efficacy evaluations in *in vivo* studies involving Parkinson's disease patients.

Conflict of Interest

The authors confirm that no conflicting financial interests or personal ties that may have impacted the work described in this publication have come to their knowledge.

Acknowledgement

The administration of Sri Ramachandra Faculty of Pharmacy, Sri Ramachandra Institute of Higher Education and Research in Tamilnadu is thanked for their assistance and encouragement.

References

- Ali, R., Alam, A., Rajput, S., & Razi, A. (2022). Pharmacotherapeutics and molecular docking studies of alpha-synuclein modulators as promising therapeutics for Parkinson's disease. *Biocell*, 46(12), 2681-2694. <https://doi.org/10.32604/biocell.2022.021224>
- Armstrong, M. J., & Okun, M. S. (2020). Diagnosis and treatment of Parkinson disease: A review. *Jama*, 323(6), 548-560. <https://doi.org/10.1001/jama.2019.22360>
- Bartels, T., Choi, J. G., & Selkoe, D. J. (2011). α -Synuclein occurs physiologically as a helically folded tetramer that resists aggregation. *Nature*, 477(7362), 107-110. <https://doi.org/10.1038/nature10324>
- Bendor, J. T., Logan, T. P., & Edwards, R. H. (2013). The function of α -synuclein. *Neuron*, 79(6), 1044-1066. <https://doi.org/10.1016/j.neuron.2013.09.004>
- Berman, H. M., Westbrook, J., Feng, Z., Gilliland, G., Bhat, T. N., Weissig, H., ... & Bourne, P. E. (2000). The protein data bank. *Nucleic Acids Research*, 28(1), 235-242. <https://doi.org/10.1093/nar/28.1.235>
- Bose, A., & Beal, M. F. (2016). Mitochondrial dysfunction in Parkinson's disease. *Journal of Neurochemistry*, 139, 216-231. <https://doi.org/10.1111/jnc.13731>
- Castro-Caldas, M., Carvalho, A. N., Rodrigues, E., Henderson, C. J., Wolf, C. R., Rodrigues, C. M. P., & Gama, M. J. (2012). Tauroursodeoxycholic acid prevents MPTP-induced dopaminergic cell death in a mouse model of Parkinson's disease. *Molecular Neurobiology*, 46(2), 475-486. <https://doi.org/10.1007/s12035-012-8295-4>
- Connolly, B. S., & Lang, A. E. (2014). Pharmacological treatment of Parkinson disease: a review. *Jama*, 311(16), 1670-1683. <https://doi.org/10.1001/jama.2014.3654>
- Cruz-Vicente, P., Gonçalves, A. M., Ferreira, O., Queiroz, J. A., Silvestre, S., Passarinha, L. A., & Gallardo, E. (2021). Discovery of small molecules as membrane-bound catechol-O-methyltransferase inhibitors with interest in Parkinson's disease: pharmacophore modeling, molecular docking and in vitro experimental validation studies. *Pharmaceuticals*, 15(1), 51. <https://doi.org/10.3390/ph15010051>
- Daina, A., Michielin, O., & Zoete, V. (2017). SwissADME: a free web tool to evaluate pharmacokinetics, drug-likeness and medicinal chemistry friendliness of small molecules. *Scientific reports*, 7(1), 42717. <https://doi.org/10.1038/srep42717>
- Dezsi, L., & Vecsei, L. (2017). Monoamine oxidase B inhibitors in Parkinson's disease. *CNS & Neurological Disorders-Drug Targets (Formerly Current Drug Targets-CNS & Neurological Disorders)*, 16(4), 425-439. <https://doi.org/10.2174/1871527316666170124165222>
- Exner, N., Lutz, A. K., Haass, C., & Winklhofer, K. F. (2012). Mitochondrial dysfunction in Parkinson's disease: molecular mechanisms and pathophysiological consequences. *The EMBO Journal*, 31(14), 3038-3062. <https://doi.org/10.1038/emboj.2012.170>
- Gnanaraj, C., Sekar, M., Fuloria, S., Swain, S. S., Gan, S. H., Chidambaram, K., ... & Fuloria, N. K. (2022). In silico molecular docking analysis of karanjin against alzheimer's and parkinson's diseases as a potential natural lead molecule for new drug design, development and therapy. *Molecules*, 27(9), 2834. <https://doi.org/10.3390/molecules27092834>
- Groiss, S. J., Wojtecki, L., Südmeyer, M., & Schnitzler, A. (2009). Deep brain stimulation in Parkinson's disease. *Therapeutic Advances in Neurological Disorders*, 2(6), 379-391. <https://doi.org/10.1177/1756285609339382>
- Guglietti, B., Mustafa, S., Corrigan, F., & Collins-Praino, L. E. (2024). Anatomical distribution of Fyn kinase in the human brain in Parkinson's disease. *Parkinsonism & Related Disorders*, 118, 105957. <https://doi.org/10.1016/j.parkreldis.2023.105957>
- Hisahara, S., & Shimohama, S. (2011). Dopamine Receptors and Parkinson's Disease. *International Journal of Medicinal Chemistry*, 2011(1), 403039. <https://doi.org/10.1155/2011/403039>
- Jost, W. H. (2022). A critical appraisal of MAO-B inhibitors in the treatment of Parkinson's disease. *Journal of Neural Transmission*, 129(5), 723-736. <https://doi.org/10.1007/s00702-022-02465-w>
- Junior, E. R. D. O., Truzzi, E., Ferraro, L., Fogagnolo, M., Pavan, B., Beggato, S., Rustichelli, C., Maretti, E., Lima, E. M., Leo, E., & Dalpiaz, A. (2020). Nasal administration of nanoencapsulated geraniol/ursodeoxycholic acid conjugate: Towards a new approach for the management of Parkinson's disease. *Journal of Controlled Release*, 321, 540-552. <https://doi.org/10.1016/j.jconrel.2020.02.033>
- Kaasinen, V., Aalto, S., Nägren, K., Hietala, J., Sonninen, P., & Rinne, J. O. (2003). Extrastriatal dopamine D2 receptors in Parkinson's disease: a longitudinal study. *Journal of Neural Transmission*, 110(6), 591-601. <https://doi.org/10.1007/s00702-003-0816-x>
- Kim, D. J., Yoon, S., Ji, S. C., Yang, J., Kim, Y. K., Lee, S., ... & Cho, J. Y. (2018). Ursodeoxycholic acid improves liver function via phenylalanine/tyrosine pathway and microbiome remodelling in patients with liver dysfunction. *Scientific reports*, 8(1), 11874. <https://doi.org/10.1038/s41598-018-30349-1>

- Kim, S., Chen, J., Cheng, T., Gindulyte, A., He, J., He, S., ... & Bolton, E. E. (2023). PubChem 2023 update. *Nucleic acids research*, 51(D1), D1373-D1380. <https://doi.org/10.1093/nar/gkac956>
- Kuriata, A., Gierut, A. M., Oleniecki, T., Ciemny, M. P., Kolinski, A., Kurcinski, M., & Kmiecik, S. (2018). CABS-flex 2.0: a web server for fast simulations of flexibility of protein structures. *Nucleic Acids Research*, 46(W1), W338-W343. <https://doi.org/10.1093/nar/gky356>
- Kwak, N., Lee, M. J., Kang, H. Y., & Lee, H. (2024). Cost-effectiveness Analysis of COMT-inhibitors as Adjuvant Treatments to Levodopa in Patients with Advanced Parkinson's Disease. *Clinical Therapeutics*, 46(9), 670-676. <https://doi.org/10.1016/j.clinthera.2024.06.016>
- Lakshmi, Y. S., Prasanth, D. S. N. B. K., Kumar, K. T. S., Ahmad, S. F., Ramanjaneyulu, S., Rahul, N., & Pasala, P. K. (2023). Unravelling the molecular mechanisms of a quercetin nanocrystal for treating potential Parkinson's disease in a rotenone model: supporting evidence of network pharmacology and in silico data analysis. *Biomedicines*, 11(10), 2756. <https://doi.org/10.3390/biomedicines11102756>
- Lim, S. Y., & Klein, C. (2024). Parkinson's disease is predominantly a genetic disease. *Journal of Parkinson's Disease*, 14(3), 467-482. <https://doi.org/10.3233/JPD-230376>
- López-Blanco, J. R., Garzón, J. I., & Chacón, P. (2011). iMod: multipurpose normal mode analysis in internal coordinates. *Bioinformatics*, 27(20), 2843-2850. <https://doi.org/10.1093/bioinformatics/btr497>
- Morris, G. M., Huey, R., Lindstrom, W., Sanner, M. F., Belew, R. K., Goodsell, D. S., & Olson, A. J. (2009). AutoDock4 and AutoDockTools4: Automated docking with selective receptor flexibility. *Journal of Computational Chemistry*, 30(16), 2785-2791. <https://doi.org/10.1002/jcc.21256>
- Müller, T. (2015). Catechol-O-methyltransferase inhibitors in Parkinson's disease. *Drugs*, 75(2), 157-174. <https://doi.org/10.1007/s40265-014-0343-0>
- O'Boyle, N. M., Banck, M., James, C. A., Morley, C., Vandermeersch, T., & Hutchison, G. R. (2011). Open Babel: An open chemical toolbox. *Journal of Cheminformatics*, 3(1), 33. <https://doi.org/10.1186/1758-2946-3-33>
- Payne, T., Sassani, M., Buckley, E., Moll, S., Anton, A., Appleby, M., ... & Bandmann, O. (2020). Ursodeoxycholic acid as a novel disease-modifying treatment for Parkinson's disease: protocol for a two-centre, randomised, double-blind, placebo-controlled trial, The'UP'study. *BMJ Open*, 10(8), e038911. <https://doi.org/10.1136/bmjopen-2020-038911>
- Qi, H., Shen, D., Jiang, C., Wang, H., & Chang, M. (2021). Ursodeoxycholic acid protects dopaminergic neurons from oxidative stress via regulating mitochondrial function, autophagy, and apoptosis in MPTP/MPP+ -induced Parkinson's disease. *Neuroscience Letters*, 741, 135493. <https://doi.org/10.1016/j.neulet.2020.135493>
- Robakis, D., & Fahn, S. (2015). Defining the role of the monoamine oxidase-B inhibitors for Parkinson's disease. *CNS Drugs*, 29(6), 433-441. <https://doi.org/10.1007/s40263-015-0249-8>
- Rosa, A. I., Duarte-Silva, S., Silva-Fernandes, A., Nunes, M. J., Carvalho, A. N., Rodrigues, E., ... & Castro-Caldas, M. (2018). Tauroursodeoxycholic acid improves motor symptoms in a mouse model of Parkinson's disease. *Molecular Neurobiology*, 55(12), 9139-9155. <https://doi.org/10.1007/s12035-018-1062-4>
- Sathe, A. G., Tuite, P., Chen, C., Ma, Y., Chen, W., Cloyd, J., ... & Coles, L. D. (2020). Pharmacokinetics, safety, and tolerability of orally administered ursodeoxycholic acid in patients with Parkinson's disease—a pilot study. *The Journal of Clinical Pharmacology*, 60(6), 744-750. <https://doi.org/10.1002/jcph.1575>
- Sharma, S., Kushwaha, K. P., & Chandra, R. (2019). Applications of BIOVIA materials studio, LAMMPS, and GROMACS in various fields of science and engineering. *Molecular dynamics simulation of nanocomposites using BIOVIA materials studio, Lammmps and Gromacs*, 329-341. <https://doi.org/10.1016/b978-0-12-816954-4.00007-3>
- Sharma, V. D., Patel, M., & Miocinovic, S. (2020). Surgical treatment of Parkinson's disease: devices and lesion approaches. *Neurotherapeutics*, 17(4), 1525-1538. <https://doi.org/10.1007/s13311-020-00939-x>
- Shtilbans, A., Reintsch, W. E., Piscopo, V. E., Krahn, A. I., & Durcan, T. M. (2024). Combination of tauroursodeoxycholic acid, co-enzyme Q10 and creatine demonstrates additive neuroprotective effects in in-vitro models of Parkinson's disease. *Frontiers in Neuroscience*, 18, 1492028. <https://doi.org/10.3389/fnins.2024.1492028>
- Song, Z., Zhang, J., Xue, T., Yang, Y., Wu, D., Chen, Z., ... & Wang, Z. (2021). Different catechol-o-methyl transferase inhibitors in Parkinson's disease: a bayesian network meta-analysis. *Frontiers in Neurology*, 12, 707723. <https://doi.org/10.3389/fneur.2021.707723>
- Stoker, T. B., & Barker, R. A. (2020). Recent developments in the treatment of Parkinson's Disease. *F1000Research*, 9, F1000-Faculty. <https://doi.org/10.12688/f1000research.25634.1>
- Sveinbjornsdottir, S. (2016). The clinical symptoms of Parkinson's disease. *Journal of Neurochemistry*, 139, 318-324. <https://doi.org/10.1111/jnc.13691>

Teo, K. C., & Ho, S. L. (2013). Monoamine oxidase-B (MAO-B) inhibitors: implications for disease-modification in Parkinson's disease. *Translational Neurodegeneration*, 2(1), 19. <https://doi.org/10.1186/2047-9158-2-19>

Vang, S., Longley, K., Steer, C. J., & Low, W. C. (2014). The unexpected uses of urso-and tauroursodeoxycholic acid in the treatment of non-liver diseases. *Global Advances In Health and Medicine*, 3(3), 58-69. <https://doi.org/10.7453/gahmj.2014.017>

Váradi, C. (2020). Clinical features of Parkinson's disease: the evolution of critical symptoms. *Biology*, 9(5), 103. <https://doi.org/10.3390/biology9050103>

Vastegani, S. M., Nasrolahi, A., Ghaderi, S., Belali, R., Rashno, M., Farzaneh, M., & Khoshnam, S. E. (2023). Mitochondrial dysfunction and Parkinson's disease: pathogenesis and therapeutic strategies. *Neurochemical Research*, 48(8), 2285-2308. <https://doi.org/10.1007/s11064-023-03904-0>

Zhang, Y., Jiang, R., Zheng, X., Lei, S., Huang, F., Xie, G., ... & Jia, W. (2019). Ursodeoxycholic acid accelerates bile acid enterohepatic circulation. *British Journal of Pharmacology*, 176(16), 2848-2863. <https://doi.org/10.1111/bph.14705>

Zhu, X. H., Lee, B. Y., Tuite, P., Coles, L., Sathe, A. G., Chen, C., ... & Chen, W. (2021). Quantitative assessment of occipital metabolic and energetic changes in Parkinson's patients, using in Vivo 31P MRS-based metabolic imaging at 7T. *Metabolites*, 11(3), 145. <https://doi.org/10.3390/metabo11030145>

Zong, Y., Li, H., Liao, P., Chen, L., Pan, Y., Zheng, Y., ... & Gao, J. (2024). Mitochondrial dysfunction: mechanisms and advances in therapy. *Signal Transduction and Targeted Therapy*, 9(1), 124. <https://doi.org/10.1038/s41392-024-01839-8>